Numerical Investigate the Effect of Turbulence Models on the CFD Computation of Submarine Resistance

Tat-Hien Le[1,2,*], Nguyen Duy Anh[1,2], Nguyen Thi Ngoc Hoa[3]

1   Ho Chi Minh City University of Technology (HCMUT), Vietnam
2   Vietnam National University Ho Chi Minh City, Vietnam
3   Ho Chi Minh City University of Transport, Vietnam

ARTICLE INFO	ABSTRACT
         	Up to now, there is no developed 'universal' turbulence model in CFD simulation, so employing an appropriate turbulence model is crucial for accurately predicting the hydrodynamics of a ship, especially for submarines. This study focuses on investigating the impact of turbulence models on the predicted results in frictional and pressure resistance components and flow features around the submarine at different ship velocities by the CFD method. Four various turbulence models consisting of the Reynolds Stress Model, realizable k-ε two-layer, standard k-ω, and SST k-ω turbulence models are investigated in this study. The obtained numerical results demonstrate variations in resistance and the flow patterns around the submarine due to the effect of turbulence model. Based on the obtained results, the paper points out that, the choice of turbulence model significantly affects the frictional resistance of the submarine and the SST K-ω turbulence model provided the highest level of accuracy in comparison with experimental data. The model employed in this research is the DARPA SUBOFF submarine model.

1. Introduction

One of the primary objectives for designers and researchers is to accurately predict the resistance of submarines at various velocities. For this purpose, in recent days, researchers worldwide have extensively employed Computational Fluid Dynamics (CFD) for evaluating the ship hydrodynamics characteristics [1-10] and particularly on the submarine hydrodynamics [11-13] due to this method offers relatively reliable results compared to experimental method [6, 14]. Furthermore, it provides the added advantage of saving time and costs, and the CFD can visualize flow detail around the ship submarine, which serves for the optimization of submarine hull form. Nevertheless, the accuracy of predicted results by the CFD method depends on many factors, including the selection of the turbulence model. Several studies have successfully utilized the CFD method with different turbulence models to predict the resistance of the ship [15-18].

---

* *Corresponding author.*
E-mail address: hienlt@hcmut.edu.vn (Tat-Hien Le)

These researchers have identified effective turbulence models for accurately estimating the resistance of the ship and have provided insightful conclusions for the selection of an appropriate turbulence model for surface ships. Concerning the submarine resistance prediction, there have been carried out by several authors [11-13, 19-22]. Tu T.N *et al.,* [11] applied the RANSE method with five different turbulence models to predict submarine resistance at different velocities. The results of this study showed that the SST k-ω turbulence model was in best agreement with the measured data. Mohammad Moonesun *et al.,*[13] used CFD method with k-ε turbulence model to investigate the effect of ratio of length to diameter on submarine resistance for minimizing the resistance. Dogancan Uzun *et al.,* [19] conducted a study influence of biofouling on submarine resistance in full-scale by using CFD method with SST k-ω turbulence model. The numerical obtained results indicated that the roughness causes considerable increase in resistance, ranging from ~36% to ~112% depending on the submarine velocities and roughness height. Dong Li *et al.,* [20] applied CFD method with a realizable k-ε turbulence model to predict submarine resistance operating near the free surface.

This study focuses on investigating the effects of four turbulence models, including Linear Pressure-Strain Reynolds Stress Model, realizable k-ε two-layer, standard k-ω, and SST k-ω on the accuracy level of predicted resistance of a submarine and the differences in flow characteristics around the submarine in submerged conditions. The submarine chosen for this research is the DARPA SUBOFF submarine in model scale. The commercial solver Star-CCM+ is utilized for the simulations.

The structure of this article is organized as follows: Section 2 provides the governing equations. In Section 3, the numerical simulation is described. Then the obtained numerical result of four various turbulence models is presented in Section 4. Finally, the conclusions derived from this research are discussed in Section 5.

2. Governing Equations
2.1 Reynolds-Averaged Navier-Stokes Equations

The application of time-averaging to the momentum and continuity equations for Reynolds Averaged Navier-Stokes equation (RANSE) is written as [23]:

$$\frac{\partial(\rho \bar{u}_i)}{\partial x_i} = 0 \tag{1}$$

and

$$V_j \frac{\partial V_i}{\partial x_j} = -\frac{1}{\rho}\frac{\partial P}{\partial x} + \frac{\partial}{\partial x_j}\left[\left(\frac{\partial V_i}{\partial x_j} + \frac{\partial V_j}{\partial x_i}\right)\right] + \frac{1}{\rho}\frac{\partial \tau_{ij}}{\partial x_j} \tag{2}$$

Where: ρ is the fluid density, x_i and x_j are the coordinates, ν presents the fluid kinematic viscosity, τ_{ij} is the Reynolds stresses tensor; *P* and V_i are the time-averaged pressure and velocity components, respectively.

2.2 Turbulence Models
2.2.1 Realizable k–ε two- layer turbulence model (RKE)

In this research, we have used four different turbulence models, which are widely used in hydrodynamics problems, consisting of the Reynolds Stress Model, realizable k-ε two-layer, standard k-ω and SST k-ω.

RKE is employed to solve the transport equations for turbulence dissipation rate (ε) and turbulence kinetic energy (k) to estimate the eddy viscosity μ_t by the below equation [16]:

$$\mu_t = \rho C_\mu f_\mu kT \tag{3}$$

Where: f_μ is a damping function and C_μ is a model coefficient.

The turbulent time scale (T) are determined by Eq. (4) as follows:

$$T = k / \varepsilon \tag{4}$$

The turbulent dissipation rate ε and transport equations for the kinetic energy k are determined as follows:

$$\frac{\partial}{\partial t}(\rho\varepsilon) + \nabla \cdot (\rho\varepsilon\overline{v}) = \nabla \cdot \left[\left(\mu + \frac{\mu_t}{\sigma_\varepsilon}\right)\nabla\varepsilon\right] + \frac{1}{T_e}C_{\varepsilon1}P_\varepsilon - C_{\varepsilon2}f_{2\rho}\left(\frac{\varepsilon}{T_e} - \frac{\varepsilon_0}{T_0}\right) + S_\varepsilon \tag{5}$$

$$\frac{\partial}{\partial t}(\rho k) + \nabla \cdot (\rho k\overline{v}) = \nabla \cdot \left[\left(\mu + \frac{\mu_t}{\sigma_k}\right)\nabla k\right] + P_k - \rho(\varepsilon - \varepsilon_0) + S_k \tag{6}$$

2.2.2 Standard k-ω (SKO) and SST K-ω (SSTKO) turbulence models

Standard k-ω (SKO) and SST K-ω (SSTKO) turbulence models are two variants of k-omega turbulence models, that solve transport equations for k and ω to calculate the μ_t. And μ_t is defined by the below equation [16]:

$$\mu_t = \rho kT \tag{7}$$

Eq. (8) and Eq. (9) estimate the turbulent time scale (T) for SKO and SSTKO, respectively, as follows:

$$T = \frac{a^*}{\omega} \tag{8}$$

$$T = \min\left(\frac{a^*}{\omega}, \frac{a_1}{SF_2}\right) \tag{9}$$

The k and ω are estimated as follows:

$$\frac{\partial}{\partial t}(\rho k) + \nabla \cdot (\rho k \overline{v}) = \nabla \cdot \left[\left(\mu + \sigma_k \mu_t \right) \nabla k \right] + P_k - \rho \beta^* f_{\beta^*} (k\omega - k_0\omega_0) + S_k \qquad (10)$$

$$\frac{\partial}{\partial t}(\rho \omega) + \nabla \cdot (\rho \omega \overline{v}) = \nabla \cdot \left[\left(\mu + \sigma_\omega \mu_t \right) \nabla \omega \right] + P_\omega - \rho \beta f_\beta (\omega^2 - \omega_0^2) + S_\omega \qquad (11)$$

Where a^*, a_1 represent the model coefficients, f_{β^*}, f_β are the free-shear and vortex-stretching modification factors, respectively, F_2 is a blending function, P_k and P_ω are production terms, σ_ω is a model coefficient, S_ω are user-specified source terms.

2.2.3 Linear Pressure-Strain Reynolds Stress Model (RSM)

Linear Pressure-Strain Reynolds Stress model (RSM) referred to as second-moment closure models, involves the direct computation of individual components of the Reynolds stress tensor R by solving the governing transport equations. These models require the solution of a total of seven equations, comprising six equations for the Reynolds stresses and an additional equation for the isotropic turbulent dissipation.

The transport equation for the Reynolds stress tensor R is [16]:

$$\frac{\partial}{\partial t}(\rho R) + \nabla \cdot (\rho R \overline{v}) = \nabla \cdot D + P + G - \frac{2}{3}\rho I \gamma_M + \underline{\phi} + \underline{\varepsilon} + S_R \qquad (12)$$

Where: P and G present the turbulence and the buoyancy production, respectively, D represents the Reynolds Stress Diffusion, and I is the identity tensor.

Reynolds Stress Diffusion D is provided below:

$$D = \left(\mu + \frac{\mu_t}{\sigma_k} \right) \nabla R \qquad (13)$$

Where: μ is the dynamic viscosity, σ_k is a model coefficient

3. Numerical Simulations
3.1 Reference Submarine Model

The submarine (DARPA SUBOFF) model is used as a simulation model in this research. This model is designed and tested by the Naval Surface Warfare Center and Tracor Hydronautics Ship Model Basin [24]. Figure 1, Table 1 depicts the main geometry with full appendages and principal characteristics of the DARPA SUBOFF submarine in model scale.
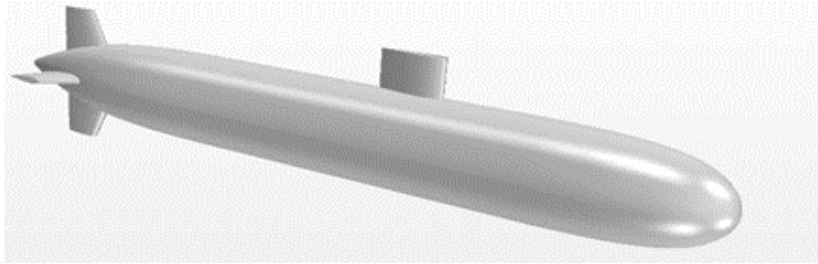
Fig. 1. Geometry of submarine DARPA SUBOFF with appendages

Table 1
Principal particulars of DARPA SUBOFF submarine in model scale

Parameters	Symbol	Unit	Value
Length overall	L_{max}	[m]	4.356
Length between perpendiculars	L_{PP}	[m]	4.261
Maximum hull diameter	D_{max}	[m]	0.508
Displacement volume	∇	[m³]	0.708
Wetted surface area	WSA	[m²]	5.998

3.2 Case Study

To investigate the effect of turbulence models on flow around submarine, the computations were conducted for the case as follows: The submarine operates in the fully submerged condition with five ship velocities V=3.050, 5.144, 6.100, 7.160, 8.230 m/s corresponding to setup in the towing tank.

3.3 Numerical Setup

The computational domain has been chosen to ensure sufficient dimensions for accurately simulating the flow around the submarine. According to the recommendation of ITTC guideline [25], for resistance simulation, the computational domain size for a submerged condition is as follows: the upstream and out-stream boundaries are extended to $1.5L_{PP}$ from the bow of the submarine and $5.0L_{PP}$ from the stern of the submarine, respectively. The top and bottom boundaries are positioned at $2.0L_{PP}$. The side boundary is located at $2.5L_{PP}$ away from the symmetry plane of the submarine. The type of boundary conditions is selected for simulating the resistance in the fully submerged condition as follows: the inlet and outlet boundaries are assigned velocity inlet and pressure outlet conditions, respectively. The bottom, top, and side boundaries are set as symmetry planes. The Submarine boundary is set as a no-slip wall boundary condition.

In this study, a trimmed mesh consisting of hexahedral elements is utilized. To accurately capture the complex flow features around the submarine, the mesh was refined around the submarine, especially at its appendages (sail and ruder fins). The prism layer mesh is employed to resolve the boundary layer. The prism layer size around the submarine hull surface is adjusted to maintain average y+ values within an acceptable range of 30-300. Specifically, the average wall y+ value of approximately 80 across all velocities (see Figure 2). This adjustment ensures proper resolution and accuracy in capturing the flow behavior near the boundary layer. Figure 3 presents the mesh generation results.
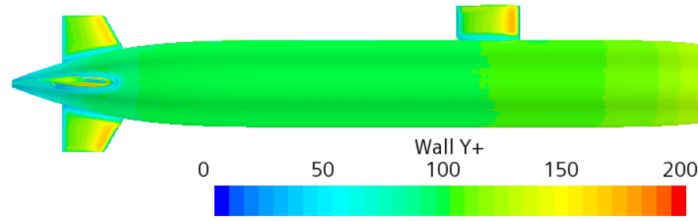
Fig. 2. Wall y+ value
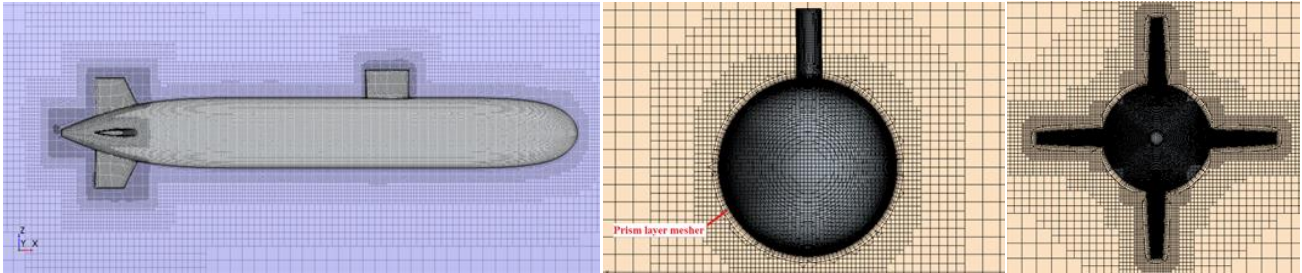
Fig. 3. Unstructured mesh around submarine

The flow around the submarine is modelled using a viscous steady Reynolds-Averaged Navier-Stokes Equations model. Single-phase are selected for submerged condition. To investigate the impact of turbulence models on predicted obtained results and the flow around the submarine, this study employs four turbulence models including RKE, SKO, SSTKO, and RSM.

3.4 Mesh Independence Study

The first step in CFD simulation is a mesh independence study. The study is conducted at the submarine velocity of 6.10 m/s with three grid sizes, including coarse, medium and fine grids with the refinement ratio r_G equal to $\sqrt{2}$ (as suggested by ITTC [26]) corresponding to the cell numbers of 0.85, 1.63 and 3.15 million cells respectively.

The convergence ratio is determined by the following formula:

$$R_k = \frac{\varepsilon_{12}}{\varepsilon_{23}} \tag{14}$$

where: $\varepsilon_{12} = (S_1 - S_2)/S_1$; $\varepsilon_{23} = (S_2 - S_3)/S_2$; S_1, S_2, and S_3 – are the solutions obtained using fine, medium, and coarse grids, respectively.

Based on formula (14), there are three possible convergence conditions, including monotonic convergence ($0 < R_k < 1$), divergence ($R_k > 1$), and oscillatory convergence ($R_k < 0$).

Table 2 and Figure 4 depict the results of the mesh independence study for four different turbulence models at the submarine velocity of 6.10 m/s. The monotonic convergence is observed for considered meshes in all of the four turbulence models due to $0 < R_k < 1$. Moreover, the simulation results (S) show good agreement with experimental data (D) especially for the fine mesh (the relative error only is 3.16%, 1.54%, 5.96% and 3.60% using RKE, SSTKO, SKO, and RSM, respectively, see Table 2), so fine mesh was used in further studies. Here, the difference between experimental data, D, and CFD simulation, S is defined as follows:

$$E\%D = \frac{(S-D)}{D} \cdot 100\%$$ (15)

Table 2
The result of mesh dependence study at submarine velocity of 6.10m/s

Parameters			RKE	SSTKO	SKO	RSM
Total resistance R_T [N]	CFD results	S1 (fine)	401.50	395.20	412.40	403.20
		S2 (medium)	403.76	396.51	414.20	405.35
		S3 (coarse)	409.25	399.42	420.25	410.62
	Experimental data	EFD	389.2			
Difference between solutions [%]	$\varepsilon_{12} = (S_1 - S_2)S_1$		0.56	0.33	0.44	0.53
	$\varepsilon_{23} = (S_2 - S_3)S_2$		1.36	0.734	1.461	1.30
Convergence ratio [-]	R_K		0.41	0.45	0.41	0.30
E%D [%]			3.16	1.54	5.96	3.60
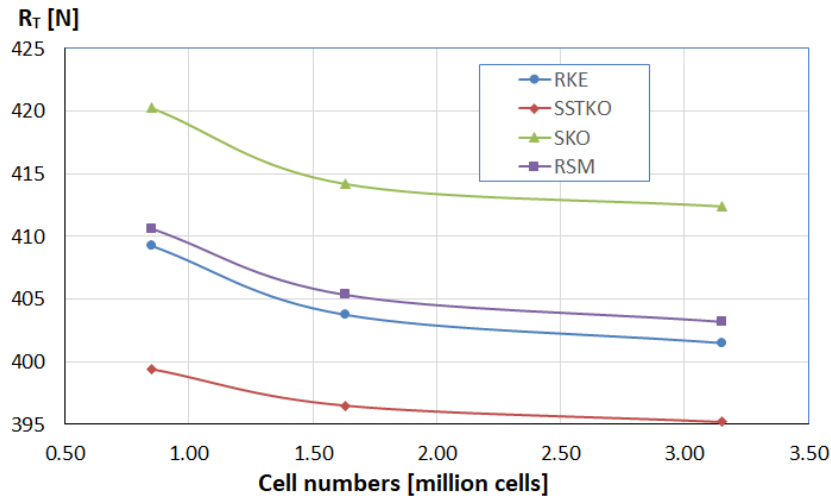
Fig. 4. Mesh independency evaluations

4. Results and Discussion

4.1 Effect of Turbulence Models on Resistance

The summary of the impact of turbulence models on the total resistance (R_T) of the submarine and its components (frictional (R_F) and pressure (R_P) components) at various ship velocities compared to experimental data [24] is presented in Table 3 and illustrated from Figures 5 to 8. The findings from Table 3 and Figures 5 to 8 reveal that:

  i. The selection of different turbulence models significantly affects the computed resistance of the submarine.
  ii. Among the various turbulence models considered, the SSTKO model provides the highest level of accuracy in comparison with experimental data. The deviation between calculated results obtained from SSTKO turbulence model and the experimental data ranged from 0.09% to 2.80% across different Froude numbers. The SKO model showed the lowest level of accuracy, with a deviation ranging from 5.31% to 7.80% in comparison with the experimental data.
  iii. The analysis of the discrepancy in resistance components resulting from various turbulence models reveals that frictional resistance is more significant than pressure

resistance components. These findings can be attributed to variations in the distribution of wall shear stress and the total pressure exerted on the submarine surface that are provided in the below parts.

Table 3
The effect of turbulence models on resistance in comparison with EFD

Turbulence models	Velocities V [m/s]	CFD computation			EFD	E%D [%]
		R_T [N]	R_F [N]	R_P [N]	R_T [N]	
RKE	3.050	106.30	90.99	15.31	102.30	3.91
	5.144	290.84	241.80	49.04	283.80	2.48
	6.100	401.50	333.65	67.85	389.20	3.16
	7.160	540.92	448.61	92.31	526.60	2.72
	8.230	698.12	578.49	119.63	675.60	3.33
SSTKO	3.050	105.20	89.85	15.35	102.30	2.83
	5.144	288.50	238.00	50.50	283.80	1.66
	6.100	395.20	326.51	68.69	389.20	1.54
	7.160	531.28	440.20	91.08	526.60	0.89
	8.230	683.15	566.52	116.63	675.60	1.12
SKO	3.050	110.28	95.13	15.15	102.30	7.80
	5.144	299.76	251.68	48.08	283.80	5.62
	6.100	412.40	346.41	65.99	389.20	5.96
	7.160	554.54	463.82	90.72	526.60	5.31
	8.230	717.68	600.65	117.03	675.60	6.23
RSM	3.050	106.56	93.24	13.32	102.30	4.16
	5.144	295.50	245.42	50.08	283.80	4.12
	6.100	403.20	336.61	66.59	389.20	3.60
	7.160	542.68	453.00	89.68	526.60	3.05
	8.230	705.52	587.24	118.28	675.60	4.43
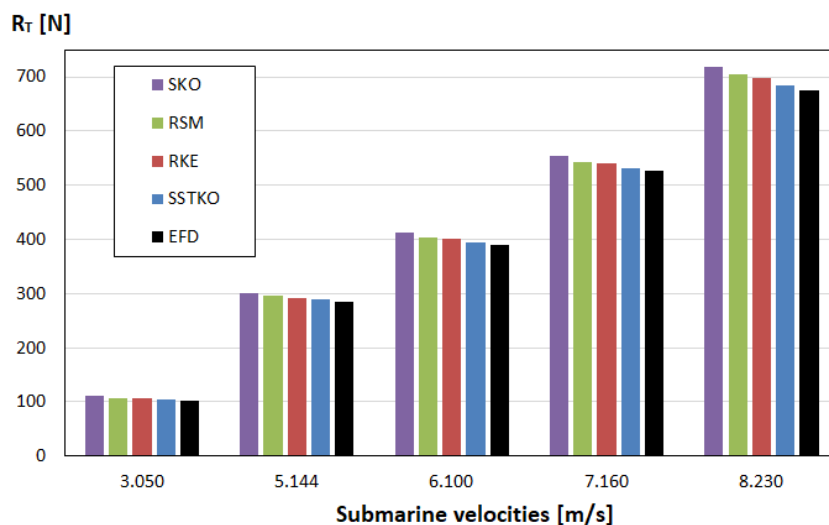
Fig. 5. The impact of turbulence models on predicted total resistance for different velocities
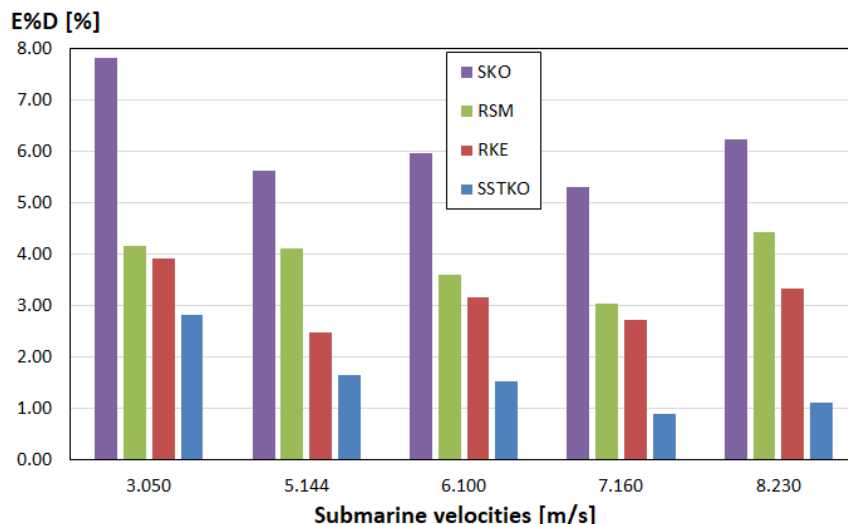
Fig. 6. The discrepancy between predicted total resistance and experimental data for different velocities with variation turbulence models
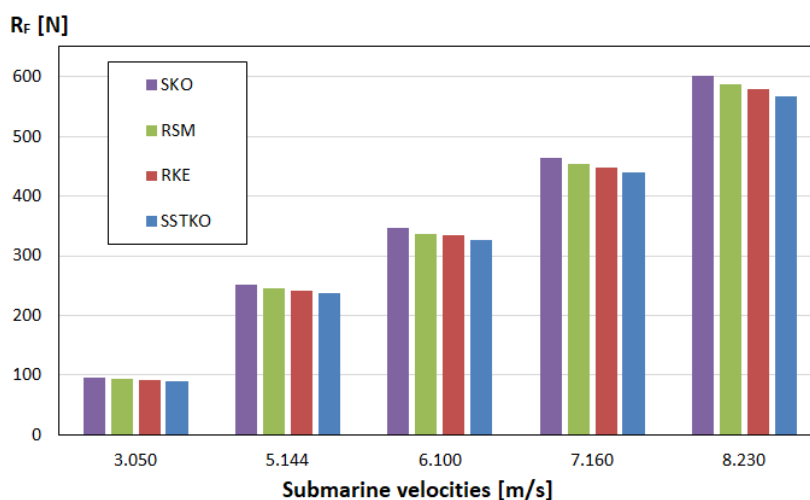
Fig. 7. The impact of turbulence models on predicted frictional resistance for different velocities
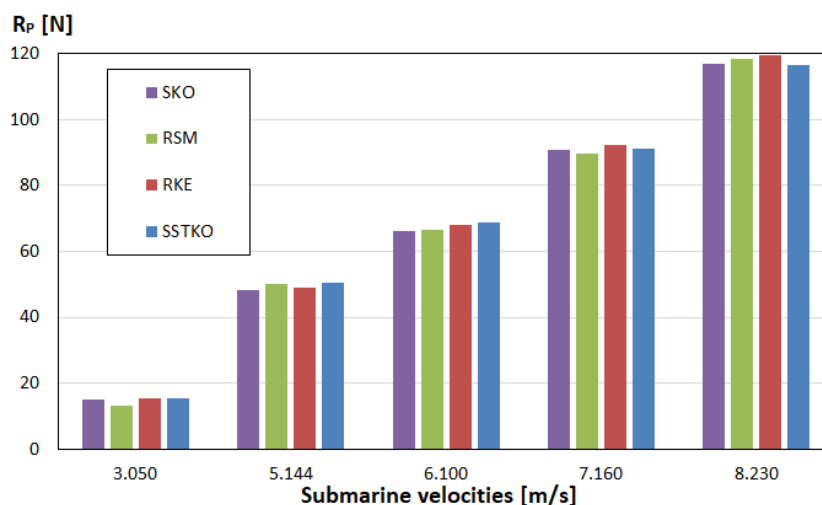
Fig. 8. The impact of turbulence models on predicted pressure resistance for different velocities

4.2 Effect of Turbulence Models on Wall Shear Stress Distribution

Figures 9 and 10 illustrate the impact of turbulence models on the wall-shear stress distribution on the hull and at horizontal sections with a Z= 0 at V=6.1m/s. These Figures demonstrate variations in the wall shear stress on the hull due to different turbulence models. It can be observed in Figure 10 that at the stern (locations from X= 0.00 to 0.6m along the submarine length) both turbulence models RKE and SKO give the lowest wall shear stress, while the biggest value belongs to RSM model. At locations from X=0.6 to X=3.90m along the submarine length, the SSTKO model gives the lowest wall shear stress, while the three remaining turbulence models give almost the same results. At the bow region from X=3.90 to 4.25m, the SSTKO and SKO models have almost the same value, while RKE model gives the lowest wall shear stress. Consequently, it is one of the reasons that lead to differences in frictional resistance components due to selection turbulence models.
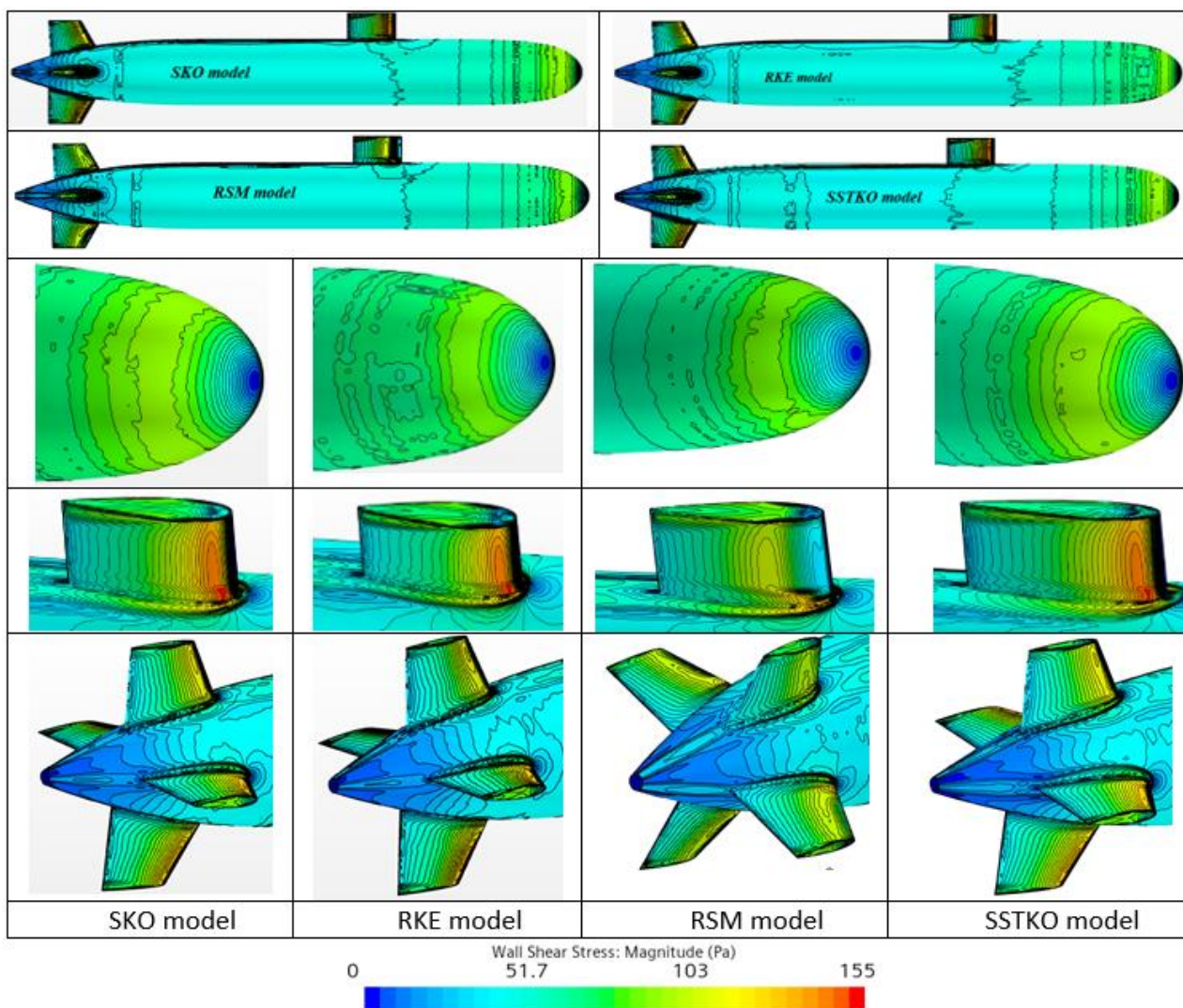
Fig. 9. Wall-shear stress distribution at V=6.1m/s

Wall shear stress [Pa]
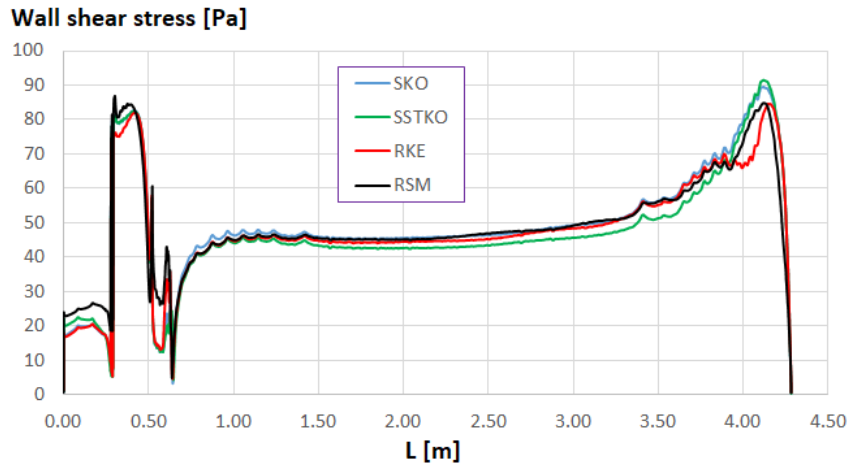
Fig. 10. Wall-shear stress distribution at horizontal sections with a Z= 0 at V=6.1m/s

4.3 Effect of Turbulence Models on Total Pressure Distribution

The impact of turbulence models on the total pressure distribution on the hull and at horizontal sections with a Z= 0 at V=6.1m/s is illustrated in Figures 11 and 12. It can be observed from these Figures, that the total pressure on the submarine is almost similar in all of the four analyzed turbulence models. This observation explains why the pressure resistance component does not vary significantly across the four turbulence models. Consequently, the total resistance is primarily influenced by changes in the components of frictional resistance.
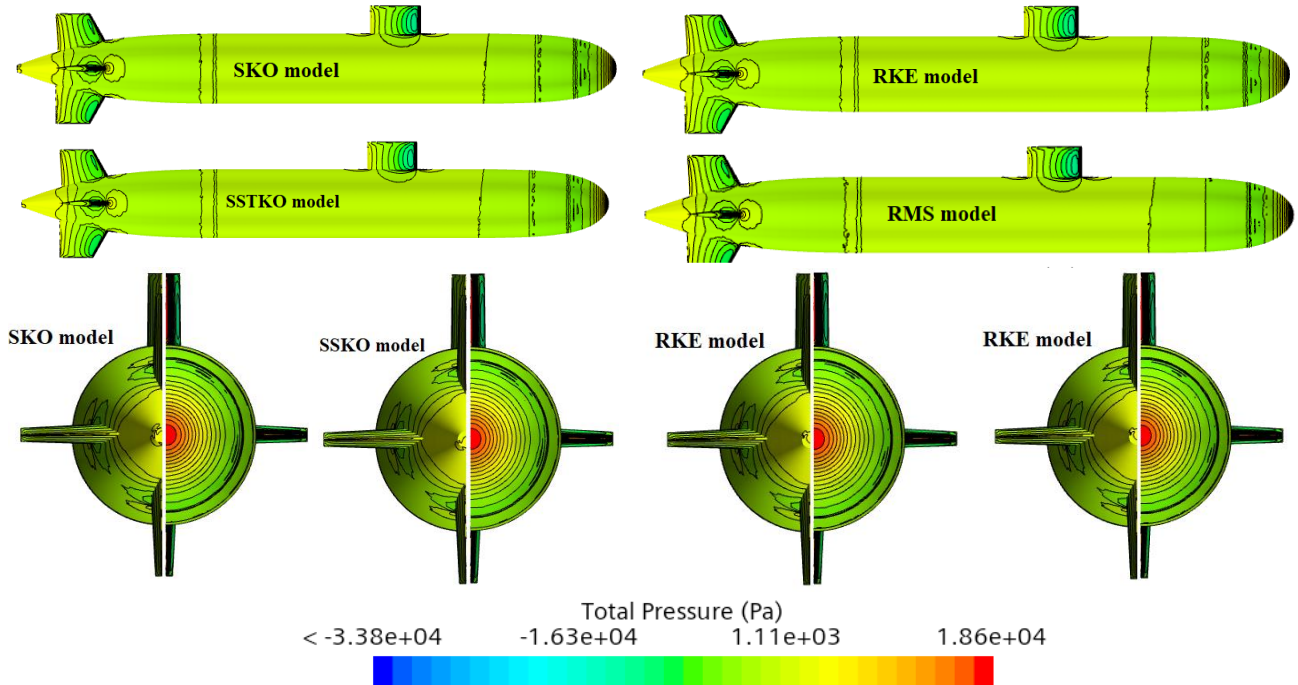
Fig. 11. Total pressure distribution at V=6.1m/s
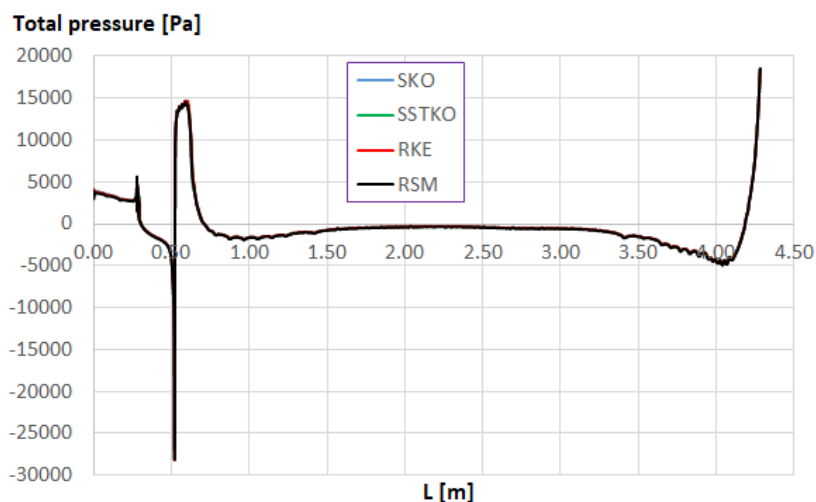
Fig. 12. Total pressure distribution at horizontal sections with a Z= 0 at V=6.1m/s

5. Conclusions

In this paper, the viscous flow around the submarine was simulated using a CFD method. To evaluate the impact of different turbulence models on submarine resistance, four popular turbulence models were employed, including Linear Pressure-Strain Reynolds Stress Model, realizable k-ε two-layer, standard k-ω, and SST k-ω. Based on the obtained results, the following conclusions can be drawn from this investigation:

  i.   The choice of turbulence model significantly affects the resistance of the submarine. Among the various turbulence models considered, the SSTKO model provided the highest level of accuracy in comparison with experimental data. The deviation between calculated results obtained from SSTKO turbulence model and the experimental data ranged from 0.09% to 2.80% across different Froude numbers. Therefore, the SSTKO turbulence model is recommended with respect to accuracy.
  ii. The choice of turbulence model mainly affects the frictional resistance component, while the component of pressure resistance is quite similar.
  iii. The choice of turbulence model significant effect on the wall shear stress distribution. Consequently, it is one of the reasons that lead to differences in frictional resistance components.

References
[1]   Ahmad Nasirudin, I Ketut Aria Pria Utama, and Andreas Kukuh Priyasambada. "CFD Analysis into the Resistance Estimation of Hard-Chine Monohull using Conventional against Inverted Bows." *CFD Letters* 15, no. 6 (2023): 54-64. https://doi.org/10.37934/cfdl.15.6.5464
[2]   Rahmat Azis Nabawi. "Study Reduction of Resistance on The Flat Hull Ship of The Semi-Trimaran Model: Hull Vane Vs Stern Foil." *CFD Letters* 13, no. 12 (2021): 32-44. https://doi.org/10.37934/cfdl.13.12.3244

[3]   I Made Ariana, Riyan Bagus Prihandanu, Dhimas Widhi Handani, and AAB Dinariyana. "Investigation of the Effects of the Pre-Duct in a Ship on Propeller–Hull Interactions Using the CFD Method." *CFD Letters* 15, no. 4 (2023): 17-30. https://doi.org/10.37934/cfdl.15.4.1730

[4]   TN Tu, NTH Phuong, VT Anh, VM Ngoc, PTT Hai, and CH Chinh. "Numerical Prediction of Ship Resistance in Calm Water by Using RANS Method." *Journal of Engineering and Applied Sciences* 13, no. 17 (2018): 7210-7214. https://doi.org/10.36478/jeasci.2018.7210.7214

[5]   Nguyen Thi Ngoc Hoa, Bich Ngoc Vu, Ngoc Tu Tran, Nguyen Manh Chien, and Tat Hien Le. "Numerical investigating the effect of water depth on ship resistance using rans CFD method." *Polish Maritime Research* (2019): https://doi.org/10.2478/pomr-2019-0046

[6]   Tran Quoc Chuan, Nguyen Kim Phuong, Tran Ngoc Tu, Mai Van Quan, Nguyen Duy Anh, and Tat-Hien Le. "Numerical Study of Effect of Trim on Performance of 12500DWT Cargo Ship Using RANSE Method." *Polish Maritime Research* 29, no. 1 (2022): 3-12. https://doi.org/10.2478/pomr-2022-0001

[7]   Hong Yee Kek, Huiyi Tan, Desmond Daniel Chin Vui Sheng, Yi Lee, Nur Dayana Ismail, Muhd Suhaimi Deris, Haslinda Mohamed Kamar, and Keng Yinn Wong. "A CFD assessment on ventilation strategies in mitigating healthcare-associated infection in single patient ward." *Progress in Energy and Environment* (2023): 35-45. https://doi.org/10.2478/pomr-2022-0001

[8]   Alaaeldeen M ElhadadAbo El-Ela. "Experimental and Cfd Resistance Validation of Naval Combatant Dtmb 5415 Model." *Journal of Advanced Research in Fluid Mechanics and Thermal Sciences* 107, no. 2 (2023): 84-102.https://doi.org/10.37934/arfmts.107.2.84102

[9]   Muhammad Nur Arham Bajuri, Djamal Hissein Didane, Mahamat Issa Boukhari, and Bukhari Manshoor. "Computational Fluid Dynamics (CFD) Analysis of Different Sizes of Savonius Rotor Wind Turbine." *Journal of Advanced Research in Applied Mechanics* 94, no. 1 (2022): 7-12. https://doi.org/10.37934/aram.94.1.712

[10]   Edi Jadmiko, Raja Oloan Saut Gurning, Muhammad Badrus Zaman, and Endang Widjiati. "Variations Rake Angle Propeller B–Series Towards Performance and Cavitation with CFD Method." *Journal of Advanced Research in Fluid Mechanics and Thermal Sciences.* 106, no. 2 (2023): 78-86. https://doi.org/10.37934/arfmts.106.2.7886

[11]   Tran Ngoc Tu, Nguyen Thi Hai Ha, Tran Viet Ha, and Nguyen Thi Ha Phuong. *Numerical Study on the Effect of Turbulence Models on RANSE Computation of Flow Around Submarine*. in *2022 9th NAFOSTED Conference on Information and Computer Science (NICS)*. 2022. IEEE. https://10.1109/NICS56915.2022.10013380

[12]   Yu-cun Pan, Huai-xin Zhang, and Qi-dou Zhou. "Numerical prediction of submarine hydrodynamic coefficients using CFD simulation." *Journal of Hydrodynamics* 24, no. 6 (2012): 840-847. https://doi.org/10.1016/S1001-6058(11)60311-9

[13]   Mohammad Moonesun, Yuri Korol, and Hosein Dalayeli. "CFD analysis on the bare hull form of submarines for minimizing the resistance." *International Journal of Maritime Technology* 3 (2015): 1-16.

[14]   Mohammad Moonesun, Mehran Javadi, Pejman Charmdooz, and Karol Uri Mikhailovich. "Evaluation of submarine model test in towing tank and comparison with CFD and experimental formulas for fully submerged resistance." *Indian Journal of Geo-Marine Sciences* 42, issue no.8 (2013): 1049-1056.

[15]   Van Nguyen, Trieu, He Van Ngo, Satowa Ibata, and Yoshiho Ikeda. "2017A-GS1-19 Effects of Turbulence Models on the CFD results of Ship Resistance and Wake." In Conference Proceedings The Japan Society of Naval Architects and Ocean Engineers 25, pp. 199-204. The Japan Society of Naval Architects and Ocean Engineers, 2017. https://doi.org/10.14856/conf.25.0_199

[16]   Tran Ngoc Tu, Vu Minh Ngoc, Nguyen Thi Thu Quynh, Nguyen Manh Chien, Nguyen Thi Hai Ha, and Nguyen Thi Ha Phuong. "Effects of Turbulence Models On RANSE Computation Of Flow Around DTMB 5415 Vessel." *Naval Engineers Journal* 133, no. 3 (2021): 137-151.

[17]   Tahara Yusuke, Hanaoka Akira, Higaki Koji, and Takai Tomohiro. "Investigation on Effective Turbulence Models for Predicting Tanker Stern Flows." The Japan Society of Naval Architects and Ocean Engineers 6 (2007): 235-246. https://doi.org/10.2534/jjasnaoe.6.235

[18]   Andrea Farkas, Nastia Degiuli, and Ivana Martić. "Assessment of hydrodynamic characteristics of a full-scale ship at different draughts." *Ocean Engineering* 156 (2018): 135-152. https://doi.org/10.1016/j.oceaneng.2018.03.002

[19]   Dogancan Uzun, Savas Sezen, Refik Ozyurt, Mehmet Atlar, and Osman Turan. "A cfd study: Influence of biofouling on a full-scale submarine." *Applied Ocean Research* 109 (2021): 102561. https://doi.org/10.1016/j.apor.2021.102561

[20]   Dong Li, Qun Yang, Lin Zhai, Zhen Wang, and Chuan-lin He. "Numerical investigation on the wave interferences of submerged bodies operating near the free surface." *International Journal of Naval Architecture Ocean Engineering* 13 (2021): 65-74. https://doi.org/10.1016/j.ijnaoe.2021.01.002

[21]   Mark Bettle, Serge L Toxopeus, and Andrew Gerber. "Calculation of bottom clearance effects on Walrus submarine hydrodynamics." *International Shipbuilding Progress* 57, no. 3-4 (2010): 101-125. https://doi.org/10.3233/ISP-2010-0065

[22] Liwei Liu, Meixia Chen, Jiawei Yu, Zhiguo Zhang, and Xianzhou Wang. "Full-scale simulation of self-propulsion for a free-running submarine." *Physics of Fluids* 33, no. 4 (2021): 047103. https://doi.org/10.1063/5.0041334

[23] JE Choi, K-S Min, JH Kim, SB Lee, and HW Seo. "Resistance and propulsion characteristics of various commercial ships based on CFD results." *Ocean engineering* 37, no. 7 (2010): 549-566. https://doi.org/10.1016/j.oceaneng.2010.02.007

[24] "Summary of DARPA Suboff Experimental Program Data. Naval Surface Warfare Center, Carderock Division (NSWCCD)."

[25] "ITTC 2011. Practical guidelines for ship CFD applications. In: Recommended procedure and Guidelines, ITTC 7.5–03-02–03.

[26] ITTC Quality Manual. "7.5-03-01-01." *Uncertainty Analysis in CFD, Verification and Validation Methodology and Procedure* (2008):